

## Radiolysis of Aqueous Solutions of 1,1- and 1,2-Dichloroethane

Simon M. Pimblott,<sup>\*,†,‡</sup> Bratoljub H. Milosavljevic,<sup>†</sup> and Jay A. LaVerne<sup>\*,†,‡</sup>

Radiation Laboratory and Department of Physics, University of Notre Dame, Notre Dame, Indiana 46556

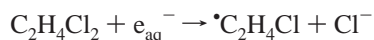
Received: July 8, 2005; In Final Form: September 7, 2005

The yields of chloride ion and molecular hydrogen were determined in the  $\gamma$ , the fast electron, and the 5 MeV helium ion radiolysis of deaerated and aerated aqueous solutions of 1,1- and 1,2-dichloroethane. In deaerated solutions irradiated with  $\gamma$ -rays or fast electrons, the yield of chloride ion increases while the yield of molecular hydrogen decreases with increasing dichloroethane concentration. These results are due to the quantitative reaction of both the hydrated electron and the hydrogen atom with the dichloroethane to produce chloride ions. The yield of chloride ions is significantly larger in aerobic than in anaerobic conditions and is dependent upon the dose rate. Formation of peroxy radicals by the reaction of molecular oxygen with chlorinated hydrocarbon radicals and their subsequent chemistry are responsible for the observed increase in chloride ions. The yield of chloride ion with 5 MeV helium ions is smaller than with  $\gamma$  irradiation, while the yield of molecular hydrogen is larger reflecting the higher density of reactive species and consequent increase in intratrack reactions in a helium ion track compared to a  $\gamma$ -ray track.

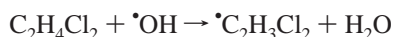
### Introduction

The radiolysis of aqueous solutions of chlorinated hydrocarbons is finding renewed interest in both natural and technological environments.<sup>1,2</sup> Radiation-induced degradation can be used in the environmental cleanup of contaminated water and can be responsible for the deleterious production of corrosive and explosive agents, like HCl and H<sub>2</sub> respectively, from chlorinated hydrocarbons in nuclear waste storage. Optimization of the conditions for radiation-induced mineralization in remediation and for nuclear waste management requires an understanding of the mechanisms and the kinetics of the reactions of the radiation-induced transients, e<sub>aq</sub><sup>-</sup>, OH radical, and H atom, with chlorinated hydrocarbons in aqueous environments.

The dichloroethanes, 1,1-DCE (CHCl<sub>2</sub>-CH<sub>3</sub>) and 1,2-DCE (CH<sub>2</sub>Cl-CH<sub>2</sub>Cl), are prototypical chlorinated hydrocarbons. They are sparingly soluble in water and purged (removed) easily from aqueous solution by bubbling. The rates for their reactions with e<sub>aq</sub><sup>-</sup>



and with OH radical



are reasonably fast with rate coefficients of  $2.3 \times 10^9 \text{ M}^{-1} \text{ s}^{-1}$  and  $2.2 \times 10^8 \text{ M}^{-1} \text{ s}^{-1}$  for 1,2-DCE, respectively.<sup>3</sup> Comparable rate coefficients are observed for 1,1-DCE.<sup>3</sup> Chloride ion yields should be predictable in deaerated solutions if these reactions are quantitative and the fate of the H atom reaction is known. Inversely, comparison of the measured chloride ion yields with known yields of e<sub>aq</sub><sup>-</sup>, OH radical, and H atom will help elucidate the reaction scheme. Aerated solutions are more complicated because of the rapid reactions of the organic radicals with

oxygen and the subsequent decay of the peroxy radicals.<sup>4,5</sup> Oxygen will also compete with DCE for reaction with the hydrated electron and H atoms. Both the hydrated electron and H atom are precursors to molecular hydrogen so modifications in their chemistry will affect H<sub>2</sub> yields. Experimental measurement of chloride ion and molecular hydrogen yields give practical information for predicting corrosion and explosive hazards and can be coupled with model studies to give a detailed understanding of the radiolysis mechanism.

A detailed experiment-with-simulation investigation of the effects of  $\gamma$ -rays, fast electrons, and 5 MeV He ions on aqueous solutions of 1,1-DCE and 1,2-DCE has been undertaken to provide fundamental information about the radiation chemistry under aerobic and under anaerobic conditions. The following section describes the experimental techniques and the modeling methodologies employed. The results obtained from varying the DCE concentration, oxygen content, radiation dose, dose rate, and type of radiation are described. A summary of the conclusions follows the discussion of the experimental and modeling results.

### Experimental Section

High purity 1,1-dichloroethane (1,1-DCE) and 1,2-dichloroethane (1,2-DCE) chromatographic standards (with no added stabilizer) from ChemService were used as received. Water was purified using an in-house H<sub>2</sub>Only system consisting of a UV lamp and several microporous ultrafilters. A kinetic trace of the decay of the hydrated electron in neat water showed no sign of impurities that could interfere in these experiments. Saturated solutions (~80 mM) were made by the appropriate addition of DCE to water in a volumetric flask sealed with a vacuum tight stopcock.<sup>6</sup> The solutions were stirred for at least 48 h to ensure solvation. Various concentrations of aerated DCE solutions were made by dilution of the saturated solution. Deaerated solutions were made by purging ultrapure nitrogen or argon through a prebubbler and then the sample cell both containing DCE solutions. The concentration of the DCE in deaerated solutions was usually about an order of magnitude lower than in aerated

<sup>†</sup> Radiation Laboratory, University of Notre Dame

<sup>‡</sup> Department of Physics, University of Notre Dame.

\* Authors for correspondence. E-mail: (S.M.P.) simon.m.pimblott.1@nd.edu; (J.A.S.) jay.a.laverne.1@nd.edu

solutions because of its volatility. DCE concentrations were determined by the decay rate of its reaction with the hydrated electron as determined in pulse radiolysis. The rate coefficients for these reactions were taken from ref 3.

$\gamma$  irradiations were performed with a Shepherd 109  $^{60}\text{Co}$  source. The dose rate was about 115 Gy/min (11.5 kRad/min) as determined by Fricke dosimetry. Radiolysis cells for chloride determination were made from 10 mm diameter Pyrex tubing. The sample was introduced into a degassed cell, flame-sealed, and irradiated. Hydrogen was determined from a cell made from a quartz cuvette with inlet and outlet for purging. Samples were irradiated at room temperature, 25 °C.

Fast electron experiments were performed using 2 ns pulses of 8 MeV electrons from the Notre Dame Radiation Laboratory linear accelerator (TB-8/16-1S linac). The linac, the spectrophotometric detection setup, and the computer-controlled data acquisition and detection systems are described in detail elsewhere.<sup>7</sup> All measurements were performed at 20 °C in a high purity silica cell of 1 cm optical path length. The radiolysis cell was sealed throughout the radiolysis to avoid evaporation of the solute.

Helium ion irradiations were performed using the FN Tandem Van de Graaff facility of the University of Notre Dame Nuclear Structure Laboratory. The window assembly and irradiation procedure were the same as reported earlier.<sup>8,9</sup> Completely stripped  $^4\text{He}$  ions were used with total beam currents of about 1 nA (charge current = particle current times particle charge,  $Z$ ). Particle energy was determined to within 0.1% by magnetic analysis and the energy loss to windows was determined from standard stopping power tables.<sup>10</sup> The samples were irradiated in a Pyrex sample cell with a thin mica window ( $\sim 6 \text{ mg/cm}^2$ ) attached. The sample cell contained a magnetic stirrer that was used throughout the radiolysis.

Chloride ions were measured using a Dionex ion chromatographic system within a few hours of the radiolysis. The ion chromatograph was calibrated with standard sodium chloride solutions. The estimated accuracy for the chloride determination is  $\pm 5\%$ . Hydrogen was determined using an inline gas chromatography technique employing an SRI 8610C instrument. The sample and prebubbler were attached to the gas stream with a four-way valve used to purge the sample and isolate it during radiolysis.

### Modeling Section

The modeling component of this study addresses two different aspects of the radiation-induced chemistry: (i) the initial nonhomogeneous reaction of the primary radiation-induced radicals and ions within the radiation track and their reactions with the DCEs and other additives; (ii) the bulk, homogeneous reaction of the oxidizing and reducing radicals and the molecular products escaping from the track. Monte Carlo track simulations employing realistic track structures and stochastic diffusion-kinetic modeling of the kinetics are performed using methods that have been described in detail previously.<sup>11–14</sup> The Monte Carlo track simulations first model the track structure of an ionizing radiation particle by following the energy attenuation of the primary ion and daughter, ejected electrons collision-by-collision. This track structure simulation is based upon energy-dependent collision cross sections for the elastic and inelastic processes of the primary ion and of energetic electrons in liquid water. The outcome is a spatially distinct track of energy transfer events. The physicochemical consequence of each energy transfer event is modeled following the methods discussed in ref 12 to produce a highly spatially nonhomogeneous distribution

of reactive radicals, ions, and excited molecules. The second component of the calculation involves the stochastic simulation of the diffusion-limited chemistry of the nonhomogeneous track of reactive species. This calculation is performed using the independent reaction times methodology,<sup>15</sup> which is based upon the independent pairs approximation that is implicit in the conventional Smoluchowski treatment of homogeneous diffusion-limited kinetics.<sup>16</sup> The relative positions of the reactants comprising the radiation track are checked for static (time zero) reaction. After allowing for the reaction of overlapping pairs of reactants, random reaction times are generated for each surviving pair from the appropriate first encounter time distribution for the pair in isolation (the application of the independent pairs approximation). The minimum time of the resulting ensemble of reaction times gives the time of the first reaction. The reacting pair is replaced by the reaction products and reaction times for these species are generated. The minimum of the new ensemble of reaction times is the next reaction time. This procedure is repeated until no reactive species remain, or a predefined cutoff time, usually 1  $\mu\text{s}$ , is reached. The basic reaction scheme used to model the radiation chemistry of water is described in ref 12 with the rate coefficients from the compilation of Buxton et al.<sup>17</sup> The rate coefficients for the reactions of the dichloroethanes with the radiation-induced water transients are from ref 3. To obtain a meaningful description of an experimental system, the averaging of  $10^2$ – $10^3$  different track chemistry simulations is necessary.

Once nonhomogeneous reactions are complete, a homogeneous distribution of reactants remains. Many of the radiation-induced products from the nonhomogeneous chemistry are reactive and can go on to participate in bulk, homogeneous reactions. These bulk, homogeneous reactions are not normally considered in conventional radiation chemistry as experiments are usually performed in the low dose regime where yield is directly proportional to dose. In the radiation chemistry associated with prolonged exposure, the radiation dose is considerable and reaction in the bulk must be considered. Modeling the radiation chemistry of aqueous solutions under high doses and dose rates involves the construction of a set of coupled differential rate equations that describes both the radiation-induced formation of reactants as a function of dose, and their reaction. The coupled equations are solved numerically using the FACSIMILE code.<sup>18</sup> A variety of studies have attempted to predict the bulk radiation chemistry of aqueous systems.<sup>19–21</sup> The calculations usually assume yields of the radiation-induced species  $e_{\text{aq}}^-$ , H, OH,  $\text{H}_3\text{O}^+$ ,  $\text{OH}^-$ ,  $\text{H}_2$ , and  $\text{H}_2\text{O}_2$  that are appropriate for escape from the radiation track in neat water. However, the yields are not independent of the irradiation conditions and depend on the radiation quality and on the track chemistry of the aqueous system under consideration. The bulk, homogeneous kinetics calculations reported here incorporate reactant formation rates derived from the yields predicted by the nonhomogeneous stochastic calculations described above. While the intratrack nonhomogeneous radiation chemistry of water involves only a limited set of fast diffusion-controlled reactions, 12 for fast electron radiolysis,<sup>22</sup> this scenario is not the case for the bulk, homogeneous chemistry.<sup>23</sup> Reactions no longer have to be fast to participate in the mechanism and slow reactions that are activation (temperature) controlled may be significant. An extended reaction scheme is required to model accurately the chemistry.

### Results and Discussion

$\gamma$  Radiolysis of Deaerated Dichloroethane Solutions. The two products measured in the radiolysis of DCE were chloride

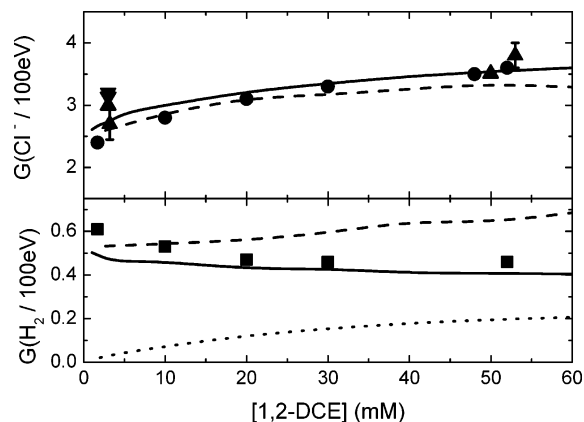
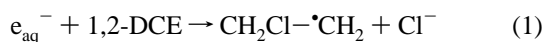
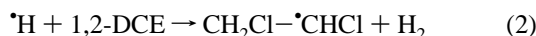


**Figure 1.** Production of chloride ion and molecular hydrogen from the  $\gamma$  radiolysis of deaerated 1,2-dichloroethane solutions. Chloride ion: experiment (●); experiment including 0.1 M ethanol (▲); experiment including 0.1 M *tert*-butyl alcohol (▼).<sup>4</sup> Molecular hydrogen: experiment (■). Simulation using reaction 2 (dashed line); simulation using reaction 2a (solid line); yield of reaction 2a (dotted line); reaction including 0.1 M ethanol (Δ); reaction including 0.1 M *tert*-butyl alcohol (▽).

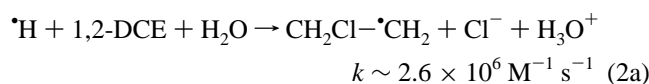
ion and molecular hydrogen. Variation of the DCE concentration gives information on the scavenging reactions of the radiation-induced transients,  $e_{\text{aq}}^-$ , OH radical, and H atom in competition with their combination reactions and diffusion in the nonhomogeneous track. The yields of chloride ion and of molecular hydrogen measured in the  $\gamma$  radiolysis of deaerated 1,2-DCE solutions are shown in Figure 1. 1,2-DCE is a scavenger for the hydrated electron



and in the gas-phase reacts with the hydrogen atom

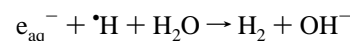


to give molecular hydrogen.<sup>24</sup> The 1,2-DCE concentration range studied, 1.7 to 52 mM, corresponds to a scavenging capacity for the hydrated electron of  $3.9 \times 10^6$  to  $1.2 \times 10^8 \text{ s}^{-1}$ , where the scavenging capacity is defined as the product of the rate coefficient and the DCE concentration. The inverse of the scavenging capacity gives an indication of the time scale of the scavenging reaction. Chloride ion yield increases with increasing 1,2-DCE concentration, while the yield of molecular hydrogen decreases. Monte Carlo track chemistry calculations of neat water including reactions 1 and 2 predict the observed increase in the yield of chloride ion. However, the absolute values calculated for the chloride ion are somewhat low. In addition, the yield of molecular hydrogen is predicted to increase with increasing 1,2-DCE concentration rather than decrease as is observed experimentally. Studies with scavengers specific for the hydrated electron show that in the low scavenging capacity limit the yield of the hydrated electron is  $\sim 2.5$  electrons/100 eV.<sup>25</sup> This value is somewhat smaller than the yield of chloride ion measured here. The measured yield of hydrogen corresponds to its spur escape yield of  $\sim 0.45$ , i.e., the microsecond yields in the absence of scavenger reactions.<sup>25</sup> These discrepancies suggests that there is an additional route for the production of chloride ion



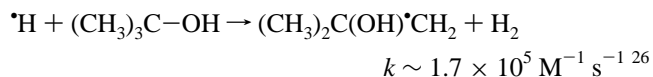
In the gas phase, the production of molecular hydrogen chloride by the abstraction of a chlorine atom is a minor channel in the reaction of H atom with 1,2-DCE, with the ratio of  $\text{H}_2$  to HCl being  $\sim 35:1$ .<sup>24</sup> Getoff previously postulated that reaction 2a was the dominant channel in aqueous solution, but without justification or support.<sup>5</sup>

Monte Carlo track chemistry calculations incorporating reaction 2a in place of reaction 2 accurately reproduce the measured experimental yields of chloride ion and hydrogen, demonstrating that reaction 2a is the dominant reaction path in aqueous solution radiolysis. Detailed examination of the reaction kinetics predicted by the stochastic simulations shows that the observed increase in the yield of chloride ion and the observed decrease in the yield of molecular hydrogen are due to an increase in the amount of reaction 2a, shown in Figure 1 to rise from 0 to  $\sim 0.2$  molecule/100 eV, and a concomitant decrease in the intra-spur reaction

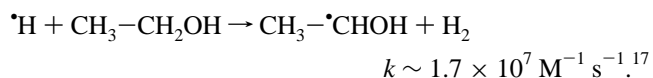


The change of reaction 2 to reaction 2a in going from the gas phase to aqueous solution reflects the thermodynamic influence of the solvation of the chloride ion and proton.

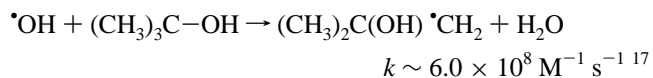
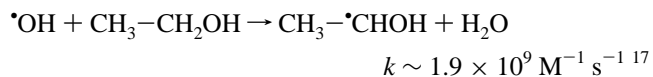
Previously, Asmus and co-workers<sup>4</sup> considered the yield of chloride from 3 mM 1,2-DCE solutions containing 0.1 M *tert*-butyl alcohol, which is a reasonable scavenger of the H atom



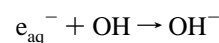
Scavenging of the H atom by *tert*-butyl alcohol should reduce the contribution of reaction 2a to the yield of chloride ion; However, their observed yield of chloride is higher than the yield measured in the absence of *tert*-butyl alcohol. Experiments performed for 3 and 50 mM 1,2-DCE solutions containing 0.1 M ethanol



support the datum of Asmus. Ethanol and *tert*-butyl alcohol, in addition to scavenging the hydrogen atom, are good scavengers of the OH radical



Monte Carlo track simulations accurately predict the measured yields of chloride ion in all three experiments. Examination of the predicted reaction kinetics reveals that the absence of a decrease in the yield of chloride ion is due to a cooperative effect.<sup>27</sup> The scavenging of the hydroxyl radical by the alcohol reduces the amount of the intraspur reaction



and increases the amount of hydrated electron available to react with 1,2-DCE.

The yields of chloride ion and of molecular hydrogen measured in the  $\gamma$  radiolysis of deaerated 1,1-DCE solutions are shown in Figure 2. Comparison of the measured yields with

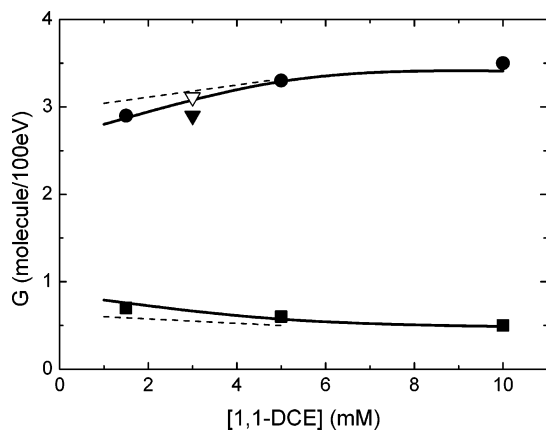
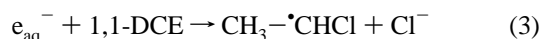
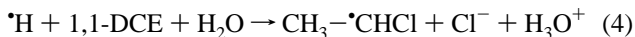


**Figure 2.** Production of chloride ion and molecular hydrogen from the  $\gamma$  radiolysis of deaerated 1,1-dichloroethane solutions. Chloride ion: experiment (●); experiment including 0.1 M *tert*-butyl alcohol (▼).<sup>4</sup> Molecular hydrogen: experiment (■). Simulation at pH 4 (solid line); simulation at pH 7 (dashed line); simulation including 0.1 M *tert*-butyl alcohol at pH 6 (▽).

the predictions of Monte Carlo track chemistry calculations show that, in deaerated solution, 1,1-DCE, like 1,2-DCE, behaves as a conventional hydrated electron scavenger



and also reacts with the hydrogen atom to give chloride ions



In the presence of 0.1 M *tert*-butyl alcohol, Asmus and co-workers measured a yield of chloride ion similar to that observed in the absence of the alcohol.<sup>4</sup> Stochastic calculations show that, as was found to be the case for 1,2-DCE, this result is due to two opposite effects, a decrease in the scavenging of H atom by 1,1-DCE, reaction 4, accompanied by a cooperative effect increasing the amount of the hydrated electron scavenged by 1,1-DCE.

**$\gamma$  and Fast Electron Radiolysis of Aerated Dichloroethane Solutions.** Previous studies found that the addition of oxygen had a significant effect on the radiolysis of aqueous DCE solutions because of the formation of peroxy radicals.<sup>4,5</sup> Aerated solutions were irradiated in this work to gain a better understanding of the mechanisms responsible for chloride ion and molecular hydrogen production in the presence of peroxy radicals. Figure 3 shows the production of chloride ion in the  $\gamma$ -ray and fast electron pulse radiolysis of aerated 1,2-DCE solutions. Two sets of irradiations were performed with each experiment giving a total dose of 175 Gy. The first set used a low dose rate (2 Gy/s)  $\gamma$ -ray source and the second employed five 35 Gy electron pulses (7 Gy/ns). In addition to the experiments performed as part of this study, the production of chloride ions from aerated solutions of 1,2-DCE was previously investigated by Getoff<sup>5</sup> and by Pikaev and co-workers.<sup>28</sup> The measured yields are very different in the four sets of experiments and depend strongly on the dose and dose rate used in the irradiations. The data of Getoff are extrapolations to the low dose limit at low dose rate (0.83 Gy/s), while Pikaev employed extremely high dose microsecond electron pulses (effective dose rate  $\sim 10^4$  Gy/s). The magnitude of the chloride ion yield varies according to  $G(\text{limiting low dose/low dose rate, ref 5}) > G(175 \text{ Gy } \gamma) > G(175 \text{ Gy electron pulse}) > G(\text{high dose/high dose rate, ref 28})$ . Standard competition kinetics suggest that under aerobic conditions the yield of chloride ion from the  $\gamma$  radiolysis

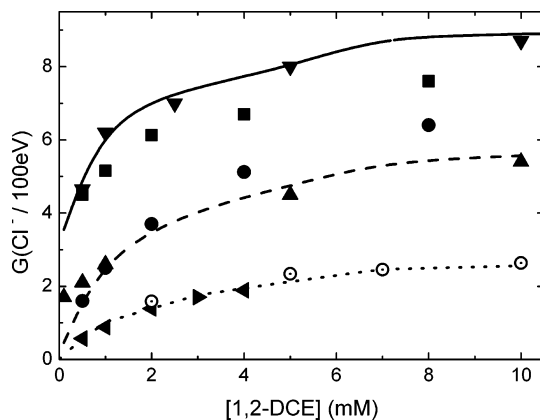
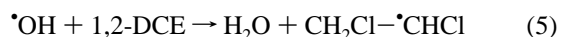


**Figure 3.** Production of chloride ion from the  $\gamma$ -ray and fast electron radiolysis of aerated 1,2-dichloroethane solutions. Experimental data: limiting low dose yield (▼);<sup>5</sup> low dose rate  $\gamma$  to a dose of 175 Gy (■); fast electron pulse radiolysis to a dose of 175 Gy (●); high dose electron pulse radiolysis (▲);<sup>28</sup> low dose rate  $\gamma$  to a dose of 175 Gy including 0.1 M ethanol (solid triangle pointing right);  $\gamma$  radiolysis including 0.1 M *tert*-butyl alcohol (solid triangle pointing left).<sup>4</sup> Simulation using complete reaction scheme (solid line); simulation excluding reaction of  $\text{CH}_2\text{Cl}-\text{OO}$  with 1,2-DCE (dashed line); predicted yield of chloride ion formed by scavenging of the hydrated electron by 1,2-DCE (dotted line) and including 0.1 M ethanol (⊙).

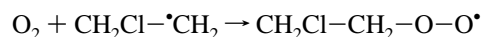
of 1,2-DCE solution is less than in deoxygenated solution. This result is expected because the dissolved molecular oxygen will efficiently compete with the 1,2-DCE for the hydrated electron and for the H atom. The predicted chloride ion yields in aerated solutions ranges from 0 to about 3.0 ions/100 eV for 1,2-DCE concentrations of 0 to  $\sim 80$  mM. The measured chloride yields in the four sets of experiments are significantly larger than the expected values.

Low-dose-rate  $\gamma$ -ray experiments were also performed incorporating 0.1 M ethanol. The yields of chloride ions from these experiments are shown in Figure 3 and are much smaller than those observed in the absence of the alcohol. As discussed earlier, ethanol rapidly scavenges radiation-induced hydroxyl radicals (and hydrogen atoms), so the reduction in the chloride ion yield when ethanol is present demonstrates that the origin of the additional chloride ions is due (at least partly) to radicals derived from the reaction of OH radicals with 1,2-DCE

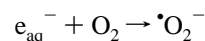


The measured yields in the experiments including ethanol and an earlier measurement of Asmus and co-workers at a 1,2-DCE concentration of about 3 mM using 0.1 M *tert*-butyl alcohol are in excellent agreement with the predictions of Monte Carlo track chemistry calculations in which the only source of chloride ion is the reaction of  $e_{\text{aq}}^-$  with 1,2-DCE. The details of the stochastic calculations reveal that the yield of chloride ion produced by the scavenging of the hydrated electron by 1,2-DCE matches the yields measured in the presence of 0.1 M ethanol.

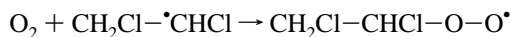
Molecular oxygen rapidly reacts with organic radicals to form peroxy radicals. In aerated solutions, the radical product of reaction 1,  $\text{CH}_2\text{Cl}-\dot{\text{C}}\text{H}_2$ , reacts with molecular oxygen to give



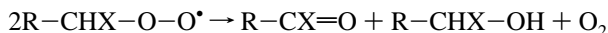
This primary peroxy radical, and the superoxide radical anion formed by the scavenging of the hydrated electron by oxygen



can abstract a hydrogen atom from 1,2-DCE, giving the  $\text{CH}_2\text{Cl}-\dot{\text{C}}\text{HCl}$  radical. This radical, which is also the product of reaction 5, reacts with molecular oxygen



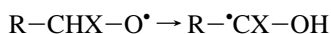
to give a secondary peroxy radical with a chlorine atom  $\alpha$  to the peroxy group. Primary and secondary peroxy radicals, like  $\text{CH}_2\text{Cl}-\text{CH}_2-\text{O}-\text{O}^{\bullet}$  and  $\text{CH}_2\text{Cl}-\text{CHCl}-\text{O}-\text{O}^{\bullet}$  respectively, have a hydrogen atom  $\alpha$  to the peroxy group and undergo bimolecular reactions of the type



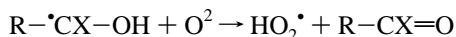
where the substituent X is either H or Cl. This reaction probably proceeds via a tetroxide intermediate,<sup>4</sup> which then undergoes rearrangement (Russell mechanism). The reaction of two peroxy radicals in this manner is not the only feasible outcome. Alternatively, two radicals may react to eliminate  $\text{O}_2$  and produce two alkoxy radicals



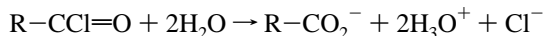
These radicals would undergo a 1,2-hydrogen shift to yield a carbon centered  $\alpha$ -hydroxy radical



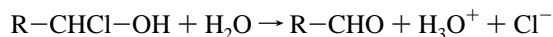
Subsequent reaction with oxygen gives



When X is a chlorine atom, the molecular product species,  $\text{R}-\text{CCl}=\text{O}$  and  $\text{R}-\text{CHCl}-\text{OH}$ , undergo rapid hydrolysis according to



and



The two feasible pathways are believed to occur in competition as is shown by considering the yield of organic acid relative to peroxy radicals.<sup>4</sup>

The predictions of Monte Carlo track chemistry simulations incorporating the reaction mechanism outlined above are included in Figure 3. These simulations consider a single isolated radiation track, and the results reflect the chemistry in the low-dose limit. The results are in excellent agreement with the experimental data of Getoff.<sup>5</sup> Examination of the details of the stochastic simulations shows that bimolecular reactions involving  $\text{CH}_2\text{Cl}-\text{CH}_2-\text{O}-\text{O}^{\bullet}$  are uncommon and reaction of  $\text{CH}_2\text{Cl}-\text{CH}_2-\text{O}-\text{O}^{\bullet}$  with 1,2-DCE dominates. Under these conditions, all the radiation-induced radicals are converted into the  $\text{CH}_2\text{Cl}-\dot{\text{C}}\text{HCl}$  radical and thence to the secondary peroxy radical,  $\text{CH}_2\text{Cl}-\text{CHCl}-\text{O}-\text{O}^{\bullet}$ . Ultimately, each radical gives a chloride ion, and the total yield of chloride ions is given by  $2(G(\text{e}_{\text{aq}}^-) + G(\text{H})) + G(\text{OH})$ . The predictions of stochastic simulations incorporating the complete reaction mechanism except for the reaction of  $\text{CH}_2\text{Cl}-\text{CH}_2-\text{O}-\text{O}^{\bullet}$  with 1,2-DCE are also shown in Figure 3. The results of these calculations are in agreement with the chloride ion yields measured in the high dose/high-dose rate pulse-radiolysis experiments of Pikaev et al.<sup>28</sup> In the high dose/high-dose rate limit, the  $\text{CH}_2\text{Cl}-\text{CH}_2-\text{O}-\text{O}^{\bullet}$  radical predominantly undergoes bimolecular reaction rather than

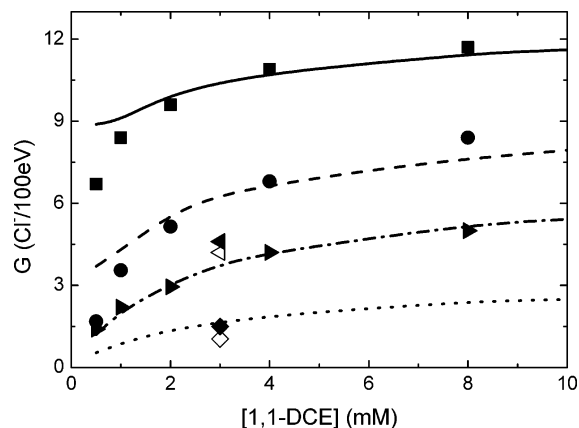
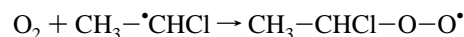


**Figure 4.** Production of chloride ion and acetate ion from the  $\gamma$ -ray and fast electron radiolysis of aerated 1,1-dichloroethane solutions. Experimental data, chloride ion: low dose rate  $\gamma$  to a dose of 175 Gy (■); fast electron pulse radiolysis to a dose of 175 Gy (●); low dose rate  $\gamma$  to a dose of 175 Gy including 0.1 M ethanol (solid triangle pointing right);  $\gamma$  radiolysis including 0.1 M *tert*-butyl alcohol (solid triangle pointing left).<sup>4</sup> Experimental data, acetate ion:  $\gamma$  radiolysis including 0.1 M *tert*-butyl alcohol (◆).<sup>4</sup> Predicted yield of chloride ion using complete reaction scheme (solid), formed by scavenging of the hydrated electron with 1,1-DCE (dotted line); including 0.1 M ethanol (dashed dot line), and including 0.1 M *tert*-butyl alcohol (open triangle pointing left). Predicted yield of acetate ion including 0.1 M *tert*-butyl alcohol (◇). Sum  $2(G(\text{reaction 3}) + G(\text{reaction 4})) + G(\text{reaction 5})$  (dashed line), i.e.,  $2(G(\text{e}_{\text{aq}}^-) + G(\text{H})) + G(\text{OH})$ .

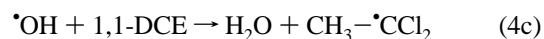
reacting with 1,2-DCE. The yield of chloride ions is therefore  $\sim G(\text{e}_{\text{aq}}^-) + G(\text{H}) + G(\text{OH})$ . The results of the experiments at 175 Gy fall between the two limits given by Getoff and Pikaev et al., with the chloride ion yield for the lower dose rate  $\gamma$  radiolysis being greater than that for electron pulses. Clearly, the effect of aeration on the production of chloride ions can be significant, but difficult to predict.

The production of chloride ion in the  $\gamma$  and fast electron pulse radiolysis of aerated 1,1-DCE solutions is shown in Figure 4. The figure compares the chloride ion yield for a dose of 175 Gy given by  $\gamma$ -rays at a rate of 2 Gy/s and by five fast electron pulses each giving a dose of 35 Gy (7 Gy/pulse). As was observed for 1,2-DCE, the yield of chloride ion is strongly dependent on the radiation dose rate and it is significantly larger than if production were solely due to the scavenging of the hydrated electron and hydrogen atom. The chloride ion yield from 1,1-DCE is higher than observed for 1,2-DCE.

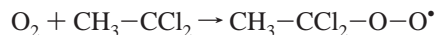
Also included in Figure 4 are measurements from  $\gamma$ -ray experiments including 0.1 M ethanol. In these experiments, hydroxyl radicals and hydrogen atoms are scavenged efficiently, and the observed chloride yield is due to the hydrated electron. Monte Carlo track chemistry simulations show that two chloride ions are produced for each scavenging reaction of 1,1-DCE with the hydrated electron. The first chloride ion comes directly from the scavenging reaction, and the second comes from the radical reactions of the secondary peroxy  $\text{CH}_3-\text{CHCl}-\text{O}-\text{O}^{\bullet}$  radical that results from the reaction of molecular oxygen with the radical  $\text{CH}_3-\dot{\text{C}}\text{HCl}$ .



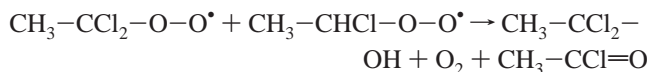
Hydrogen atoms, like hydrated electrons, give two chloride ions in the absence of ethanol. The hydroxyl radical reacts with 1,1-DCE



to give the radical  $\text{CH}_3\text{-}\dot{\text{C}}\text{Cl}_2$ . In aerated solution, this radical reacts with molecular oxygen to give a tertiary peroxy radical



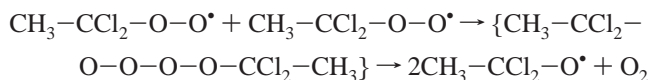
that will not abstract a hydrogen atom from a C-H bond in 1,1-DCE,<sup>4</sup> but will participate in the radical reactions. Reaction with the secondary peroxy radical  $\text{CH}_3\text{-CHCl-O-O}\cdot$  gives molecular products



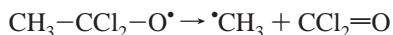
that undergo rapid hydrolysis



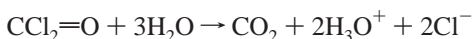
producing chloride ions. The reaction of two  $\text{CH}_3\text{-CCl}_2\text{-O-O}\cdot$  radicals yields two alkoxy radicals via a tetraoxide intermediate.



The alkoxy radical,  $\text{CH}_3\text{-CCl}_2\text{-O}\cdot$ , can abstract a hydrogen atom from a hydrocarbon and hydrolysis of the resulting  $\alpha$ -chloro alcohol,  $\text{CH}_3\text{-CCl}_2\text{-OH}$ , is fast.<sup>4</sup> Alternatively, the alkoxy radical may undergo cleavage



The molecular products of the radical cleavage reactions will subsequently undergo hydrolysis



giving chloride ions. Furthermore, the chlorine atom and the methyl radical may abstract a hydrogen atom from 1,1-DCE initiating a chain process. The observed chloride ion yield from the  $\gamma$  radiolysis of 1,1-DCE reflects a competition between two first-order processes: H abstraction and C-X bond cleavage. If the former were dominant, then the yield of chloride ions would be independent of dose. The observed yield is, however, dose dependent. This dependence is due to the competition between chain propagation and chain termination in the chemistry of the chlorine atom (or methyl radical). The expected yield of chloride ions according to this mechanism is

$$G(\text{Cl}^-) > 2(G(e_{\text{aq}}^-) + G(\text{H})) + G(\text{OH})$$

The predictions of Monte Carlo track chemistry simulations are included in Figure 4. In the low dose limit, the measured yield of chloride ions is approximately  $2(G(e_{\text{aq}}^-) + G(\text{H})) + G(\text{OH})$  and only short chain processes occur. Under high dose conditions, the measured yield of chloride ions is approximately  $2(G(e_{\text{aq}}^-) + G(\text{H})) + G(\text{OH})$ . Stochastic calculations suggest that no significant chain processes are initiated, as the density of reactants is sufficiently high that radical recombination (termination) reactions dominate.

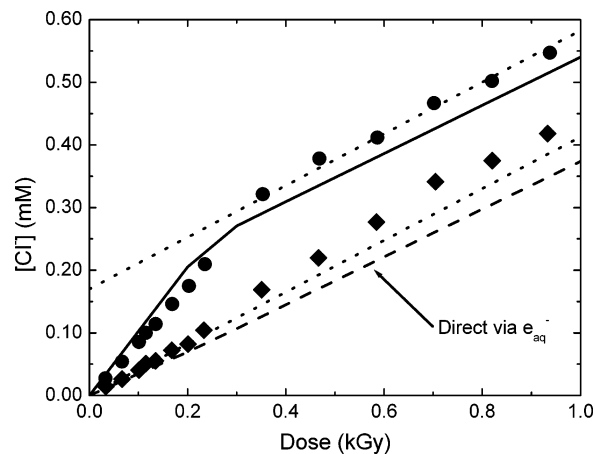


**Figure 5.** Effect of dose on the production of chloride ion in the  $\gamma$  radiolysis of aerated 80 mM 1,2-DCE solution. Experiment: aerated solution ( $\bullet$ ); solution including 80 mM ethanol ( $\blacklozenge$ ). Calculation: aerated solution (solid line); direct scavenging of the hydrated electron by 1,2-DCE (dashed line). Fit to low dose data from solutions including 0.1 M ethanol and translation of this line by 0.17 mM (dotted lines).

#### Effect of Dose on the $\gamma$ Radiolysis of Dichloroethane Solutions.

The previous section showed that dose had an effect on the observed chloride ion yield so a more thorough examination was performed. Figure 5 presents the production of chloride ion in the  $\gamma$  radiolysis of aerated 80 mM 1,2-DCE solutions at a dose rate of 115 Gy/min in the absence and in the presence of 0.1 M ethanol. Under aerobic conditions in the absence of ethanol, the concentration of chloride ions increases linearly with dose, but with two functional dependences. In the low-dose limit below about 300 Gy, the yield is  $\sim 8.9$  and in the high-dose limit it is  $\sim 4.3$  chloride ions/100 eV. The latter value is about the same yield of chloride ions in deaerated solutions. In the presence of 0.1 M ethanol, the increase in the concentration of chloride ions is approximately linear with dose. The yield of chloride ions in the presence of ethanol is  $\sim 4.3$  chloride ions/100 eV, which is the same as the yield of chloride ion in the high dose limit in the absence of ethanol.

Deterministic kinetic calculations were used to elucidate the mechanisms responsible for the observed dose dependences in the radiolysis of 1,2-DCE. The calculated results are presented in Figure 5. They reveal that the dose dependence of the yield of chloride ions in aerated solution in the absence of ethanol is due to consumption of molecular oxygen in the experimentally "isolated" system. The depletion of oxygen results in a change in the mechanism for the production of chloride ion. As discussed in the previous section the presence of oxygen leads to the formation of the peroxy radical  $\text{CH}_2\text{Cl-CHCl-O-O}\cdot$  and a subsequent high yield of chloride ions. Depletion of oxygen eliminates the contribution of this pathway to the production of chloride ions. Ultimately, the only sources of chloride ions are the scavenging reactions of 1,2-DCE with the hydrated electron and the hydrogen atom, as in deaerated solutions.

The production of chloride ions in the  $\gamma$  radiolysis of deaerated 10 mM 1,2-DCE solutions to very high doses of about 150 kGy is shown in Figure 6. The rate of production of chloride ions is very dependent on the absorbed dose. The inset in Figure 6 shows the decrease in the yield of chloride ions as a function of dose in addition to the change in the pH of the solution due to the formation of  $\text{H}_3\text{O}^+$  as the counterion to chloride. Also included in the figure are the predictions of a stochastic diffusion-kinetic calculation and deterministic modeling of the chemistry using a reaction scheme that includes the radiation

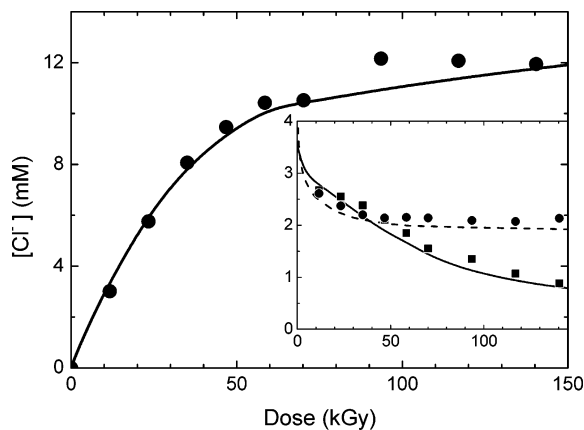


**Figure 6.** Effect of dose on the production of chloride ion in the  $\gamma$  radiolysis of deaerated 10 mM 1,2-DCE solution. Experiment: deaerated solution ( $\bullet$ ). Calculation: solid line. Inset:  $G(\text{Cl}^-)$ , ions/100 eV measured ( $\blacksquare$ ), calculated (solid line); pH measured ( $\bullet$ ), calculated (dashed line).

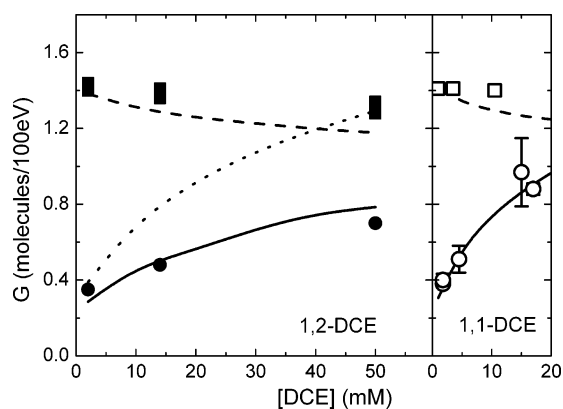


**Figure 7.** Yield of chloride ions and molecular hydrogen from 5 MeV helium ion radiolysis of deaerated 1,2-DCE and 1,1-DCE solutions. Left frame, 1,2-DCE. Experiment: chloride ion (solid line); molecular hydrogen (dashed line); predicted yield of scavenged hydrated electrons and hydrogen atoms (dotted line). Right frame, 1,1-DCE. Experiment: chloride ion ( $\circ$ ); molecular hydrogen ( $\square$ ). Simulation: chloride ion (equivalent to yield of scavenged hydrated electrons and hydrogen atoms) (dashed line); molecular hydrogen (solid line).

chemistry of the residues from the fundamental reactions discussed thus far. Deterministic calculations were performed using the yields predicted by the stochastic calculation at 10 ns. The deterministic calculations employing the yields predicted by stochastic simulation are in good agreement with the experimental data. The results show that the change in the rate of production of chloride ions and the decrease in pH reflect the destruction of 1,2-DCE and its chlorine containing residues until all of the dissolved chlorine is in the form of chloride ions. The counterion of the chloride ion is  $\text{H}_3\text{O}^+$ , hence the decrease in pH.

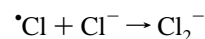
**Helium Ion Radiolysis of Dichloroethane Solutions.** The yields of chloride ion in the  $\gamma$  radiolysis of deaerated DCE solutions can be predicted from the chemistry shown in the previous sections and the yields of  $e_{\text{aq}}^-$ , OH radical, and H atom. Heavy ion radiolysis is characterized by tracks containing high concentrations of these water radiolysis products.<sup>29</sup> Combination reactions in the track decrease the radical yields escaping into the bulk medium and thereby available to react with DCE. Other high order reactions can also take place in the heavy ion track. For instance, reactions of OH radicals with the  $\text{Cl}^-$  formed in the reaction of the hydrated electron with DCE are not important in  $\gamma$  radiolysis, but might be significant in heavy ion radiolysis.

Since many radioactive waste materials are  $\alpha$  particle emitters, studies were performed with helium ions of 5 MeV.

The yields of chloride ions and molecular hydrogen from the 5 MeV helium ion radiolysis of deaerated 1,2-DCE and 1,1-DCE solutions are shown in Figure 7. In the left-hand frame for 1,2-DCE, the measured yield of chloride ion is much smaller (about a factor of 2) than the yield of ammonium cation produced from glycylglycine solutions of the same scavenging capacity for the hydrated electron.<sup>30</sup> Glycylglycine scavenges the hydrated electron quantitatively, and since 1,2-DCE scavenges both the hydrated electron and the hydrogen atom producing chloride ion, a higher yield of chloride ion than ammonium cation is expected. Stochastic diffusion-kinetic calculations qualitatively reproduce the helium-ion radiolysis kinetics of glycylglycine solutions. However, calculations incorporating only the scavenging reactions of 1,2-DCE predict significantly higher yields of chloride ions than are measured. This discrepancy suggests that hydrated electron and the hydrogen atom do not react quantitatively with 1,2-DCE, or the chloride ion undergoes subsequent intratrack reaction. Inclusion of the intratrack chemistry of the chloride ion



and



leads to the predicted yield of chloride ion matching that measured experimentally for 5 MeV helium ions. The density of radiation-induced reactants in a helium ion track is much higher than in a  $\gamma$ -ray track. Consequently, the intratrack chemistry of the chloride ion is not important in  $\gamma$  radiolysis because of the lower local concentration of hydroxyl radicals, which preferentially react with 1,2-DCE. The yield of molecular hydrogen predicted by stochastic simulation is in excellent agreement with the experimental measurements. This agreement supports the hypothesis that free hydrogen atoms abstract chlorine atoms rather than hydrogen atoms from 1,2-DCE.

The measured yield of chloride ion shown in the right-hand frame of Figure 7 for 1,1-DCE solutions is larger than was measured for 1,2-DCE and is comparable to the expected yield of hydrated electrons scavenged, i.e., the yield of ammonium cation obtained in the radiolysis of glycylglycine solutions of the same scavenging capacity. The yields of molecular hydrogen obtained from the radiolysis of 1,1- and 1,2-DCE are the same. Also shown in the figure are the predictions of stochastic diffusion kinetic calculations. There is good agreement between calculation and experiment without needing to incorporate the reaction of the hydroxyl radical with the chloride ion, suggesting that the reactivity of the radical  $\text{CH}_3\text{-}\cdot\text{CHCl}$  with the hydroxyl radical is larger than that of chloride ion and is significantly larger than that of  $\text{CH}_2\text{Cl-}\cdot\text{CH}_2$ . For both  $\text{CH}_3\text{-}\cdot\text{CHCl}$  and  $\text{CH}_2\text{Cl-}\cdot\text{CH}_2$ , the reaction with hydroxyl probably involves hydrogen atom abstraction giving water and vinyl chloride.

Figure 8 details the production of chloride ion and molecular hydrogen from the 5 MeV helium ion radiolysis of aerated 1,2-DCE solutions. As in  $\gamma$  radiolysis, chloride ion yields are much greater in aerated solutions than in deaerated ones. Stochastic diffusion-kinetic calculations qualitatively reproduce chloride ion yield using the same chemistry as in  $\gamma$  radiolysis and including the OH radical reaction with chloride ion as discussed above. However, the agreement between model calculations and experimental molecular hydrogen yields are not good. The error is about 20%, and it could be due to an unknown reaction of

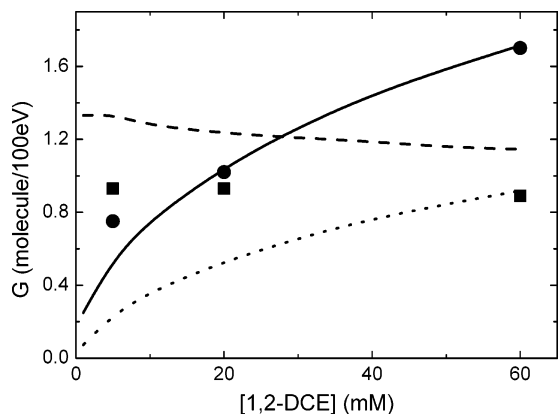


**Figure 8.** Yield of chloride ions and molecular hydrogen from 5 MeV helium ion radiolysis of aerated 1,2-DCE solutions. Experiment: chloride ion (solid line); molecular hydrogen (dashed line); predicted yield of scavenged hydrated electrons and hydrogen atoms (dotted line).

molecular hydrogen with a radiation produced radical. Because of its high volatility only one concentration value at 8 mM 1,1-DCE could be examined in deaerated solutions. The result was a yield of 1.33 and 1.3 molecule/100 eV for molecular hydrogen and chloride ion, respectively. Both of these values agree with the results predicted by the stochastic diffusion-kinetic calculations.

### Conclusions

In deaerated solutions, 1,2- and 1,1-DCE quantitatively reacts with the hydrated electron at close to diffusion-controlled rates to give chloride ion. The hydrogen atom is also scavenged by the DCEs to give chloride ion in contrast to the gas-phase reaction where the product of the abstraction reaction is molecular hydrogen. Consequently, the observed yield of chloride is a measure of the total radiation-induced yield of reducing radicals rather than hydrated electrons alone.

Radiolysis of 1,2- and 1,1-DCE solutions under aerated conditions gives significantly larger yields of chloride ions than in the absence of oxygen. This additional production derives from the chemistry of peroxy radicals formed by the addition of molecular oxygen to the radicals generated by the reactions of the primary radiation-induced radicals,  $e_{aq}^-$ , H, and OH, with the DCEs. The yield of chloride ion is strongly dependent upon the dose rate. In 1,2-DCE, this dependence is due to the competition between first- and second-order reactions of the peroxy radicals, while in 1,1-DCE it reflects the competition between the propagation and termination reactions of a chain process involving chlorine atoms.

Under the experimental conditions where the amount of oxygen is limited, the consumption of molecular oxygen with high doses of radiation has a marked effect on the rate of production of chloride ions. The change corresponds to the (expected) shift from aerobic to anaerobic conditions. When DCE solutions are irradiated to extremely high doses, complete conversion from covalently bound chlorine atoms in C-Cl bonds to aqueous chloride ions is found.

Helium ion radiolysis of deaerated 1,2-DCE solutions gives smaller chloride ion yields than expected from previous studies using glycylglycine as a hydrated electron scavenger. The lower yield observed reflects the intratrack reaction of chloride ions with hydroxyl radicals within the dense heavy ion track. In contrast, the yields of chloride ion obtained from 1,1-DCE solutions corresponds to the expected yields based on the production of the hydrated electron and H atom. The difference between 1,2- and 1,1-DCE suggests that the reactivity of the residue species with OH radical follows the order:  $CH_3-\dot{C}HCl > Cl^- > CH_2Cl-\dot{C}H_2$ .

**Acknowledgment.** This research was supported by the Office of Science (BER), U.S. Department of Energy, Grant No. DE-FG02-04ER63744. This contribution is NDRL-4616 from the Notre Dame Radiation Laboratory.

### References and Notes

- Nickelsen, M. G.; Cooper, W. J.; Secker, D.A.; Rosocha, L. A.; Kurucz, C. N.; Waite, T. D. *Radiat. Phys. Chem.* **2002**, *65*, 579.
- National Research Council, *Research Opportunities for Managing the Department of Energy's Transuranic and Mixed Wastes*; National Academy Press: Washington, DC, 2002.
- Milosavljevic, B. H.; LaVerne, J. A.; Pimblott, S. M. *J. Phys. Chem. A* **2005**, *109*, 7751.
- Lal, M.; Monig, J.; Asmus, K.-D. *J. Chem. Soc., Perkin Trans. 2* **1987**, 1639.
- Getoff, N. *Radiat. Phys. Chem.* **1990**, *35*, 432.
- Yalkowsky, S. H.; He, Y. *Handbook of Aqueous Solubility Data*; CRC Press: Boca Raton, FL, 2003.
- Hug, G. L.; Wang, Y.; Schoeneich, C.; Jiang, P.-Y.; Fessenden, R. W. *Radiat. Phys. Chem.* **1999**, *54*, 559.
- LaVerne, J. A.; Schuler, R. H. *J. Phys. Chem.* **1987**, *91*, 5770.
- LaVerne, J. A.; Schuler, R. H. *J. Phys. Chem.* **1987**, *91*, 6560.
- Ziegler, J. F.; Biersack, J. P.; Littmark, U. *The Stopping Power and Range of Ions in Solids*; Pergamon: New York, 1985.
- Pimblott, S. M.; LaVerne, J. A.; Mozumder, A. *J. Phys. Chem. A* **1996**, *100*, 8595.
- Pimblott, S. M.; LaVerne, J. A. *J. Phys. Chem. A* **1997**, *101*, 5828.
- Pimblott, S. M.; LaVerne, J. A. *J. Phys. Chem. A* **1998**, *102*, 2967.
- Pimblott, S. M.; LaVerne, J. A. *J. Phys. Chem. A* **2002**, *106*, 9420.
- Clifford, P.; Green, N. J. B.; Oldfield, M. J.; Pilling, M. J.; Pimblott, S. M. *J. Chem. Soc. Faraday Trans. 1* **1986**, *82*, 2673.
- Rice, S. A. In *Diffusion-limited Reactions. Comprehensive Chemical Kinetics*; Bamford, C. H., Tipper, C. F. H., Compton, R. G., Eds.; Elsevier: Amsterdam, 1985; Vol. 25.
- Buxton, G. V.; Greenstock, C. L.; Helman, W. P.; Ross, A. B. *J. Phys. Chem. Ref. Data* **1988**, *17*, 513.
- Chance, E. M.; Curtis, A. R.; Jones, I. P.; Kirby, C. R. Report AERE-R 8775; AERE: Harwell, U.K., 1977.
- Burns, W. G.; Sims, H. E.; Goodall, J. A. B. *Radiat. Phys. Chem.* **1984**, *23*, 143.
- Nucl. Technol.* **1995**, *109*, 373.
- Pastina, B.; LaVerne, J. A. *J. Phys. Chem. A* **2001**, *105*, 9316.
- Schwarz, H. A. *J. Phys. Chem.* **1969**, *73*, 1928.
- Elliot, A. J.; Chenier, M. P. *J. Nucl. Mater.* **1992**, *187*, 230.
- Knyazev, V. D. *J. Phys. Chem. A* **2002**, *106*, 11603.
- LaVerne, J. A.; Pimblott, S. M. *J. Phys. Chem.* **1991**, *95*, 3196.
- Smaller, B.; Avery, E. C.; Remko, J. R. *J. Chem. Phys.* **1971**, *55*, 2414.
- Pimblott, S. M.; LaVerne, J. A. *J. Phys. Chem.* **1992**, *96*, 8904.
- Kartasheva, L. I.; Zhestkova, T. P.; Chulkov, V. N.; Didenko, O. A.; Pikaev, A. K. *High Energy Chem. (Transl. of Khim. Vys. Energ.)* **1996**, *30*, 230.
- LaVerne, J. A. In *Charged Particle and Photon Interactions with Matter*; Mozumder, A., Hatano, Y., Eds.; Marcel Dekker: New York, 2004; Chapter 14.
- LaVerne, J. A.; Yoshida, H. *J. Phys. Chem.* **1993**, *97*, 10720.